

A new parametrization of the boundary layer forcing in the deep convection scheme of Bechold et al., 2014 and its implementation in ARPEGE/ALADIN physics

Siham SBII, Noureddine Semane and Yves Bouteloup

Numerical Modelling section, National Center for Meteorological Researches

12-16 April 2021

- Bechtold et al. 2014 nonequilibrium Closure for Deep convection
- Our motivation : why there is an overestimation of precipitation with B14 in some cases ?
- Reformulation of Boundary Layer Forcing
- Its implementation in ARPEGE/ALADIN Physics
- First results on ALADIN-Morocco , ALADIN-NORAF (and ARPEGE ?)

The task of the Convection Parametrization

To calculate the collective effects of an ensemble of convective clouds in a model column as a function of grid-scale variables.

In IFS, the terms Q_{1c} , Q_{2c} and Q_{3c} measure the convective effects on static energy, humidity and horizontal wind :

$$\left\{ \begin{array}{l} Q_{1c} = Q_1 - Q_R = L_v(\bar{c} - \bar{e}) - \frac{\partial \overline{\omega' s'}}{\partial p} \\ Q_{2c} = L_v(\bar{c} - \bar{e}) - L_v \frac{\partial \overline{\omega' q'}}{\partial p} \\ Q_{3c} = -\frac{\partial \overline{\omega' \vec{v}'_h}}{\partial p} \end{array} \right. \quad (1)$$

The main characteristics of the IFS Convection scheme

The main characteristics of the IFS Convection are as follows :

- bulk mass-flux scheme
- entraining/detraining plume cloud model
- three types of convection : deep, shallow and mid-level - mutually exclusive trigger of convection based on parcel instability, parcel velocity, and parcel initial t and q perturbation
- saturated downdraughts
- simple microphysics scheme
- convective (cloud base mass flux) closure dependent on type of convection : CAPE adjustment for deep convection, PBL equilibrium for shallow convection and large scale omega for mid-level convection
- strong link to cloud parametrization-convection provides source for cloud condensate

The convective available potential energy (CAPE) closure

Instead of the vertical integral of an entraining ascending air parcel :

$$\text{CAPE} = g \int_{z_b}^{z_t} \frac{T_{vc} - \overline{T_v}}{\overline{T_v}} dz \quad (2)$$

the density-weighted buoyancy is used

$$\text{PCAPE} = - \int_{p|_{z=z_b}}^{p|_{z=z_t}} \frac{T_{vc} - \overline{T_v}}{\overline{T_v}} dp; \quad dp = \rho g dz \quad (3)$$

where z is height, z_b is the cloud base, z_t is the cloud top, T_v is the virtual temperature and g is gravity, ρ the density, the subscript c denotes convective values, and the bar denotes large-scale or grid-mean values.

The closure assumes that an equilibrium exists between the large-scale and boundary-layer forcing (generating the PCAPE) and convection (reducing the PCAPE).

The *CAPE*-adjusted closure of Bechtold et al. 2014

Assuming that convection acts to remove *PCAPE* over a convective adjustment timescale τ , the *CAPE*-adjusted closure relaxes the large-scale forcing *PCAPE* to a reference value $PCAPE_{bl}$ over τ as follows :

$$\left. \frac{\partial PCAPE}{\partial t} \right|_c = - \frac{PCAPE - PCAPE_{bl}}{\tau} \quad (4)$$

$PCAPE_{bl}$ is computed as follows :

$$PCAPE_{bl} = - \frac{\tau_{bl}}{T_\star} \int_{p|_{z=0}}^{p|_{z=z_b}} \left. \frac{\partial \overline{T_v}}{\partial t} \right|_{bl} dp$$

$$\tau_{bl} = \frac{z_t - z_b}{\overline{w}_c} \quad \text{continental boundary layer} \quad (5)$$

$$\tau_{bl} = \frac{z_b}{\overline{u}_{bl}} \quad \text{oceanic boundary layer}$$

where $p|_{z=0}$ is the surface pressure, T_\star is a temperature parameter (set to 1K $T_\star = C_p^{-1} gH$), \overline{w}_c is the average vertical wind speed in the cloud layer and \overline{u}_{bl} is the average horizontal wind speed in the boundary layer.

General motivations

- Representing convection at **the right time** and **place** is crucial to the realistic simulation of atmospheric variability
- As shown in Bechtold et al. 2014, the B14 scheme *better represents the mainly surface-driven convection over ... the Atlas Mountains, a situation that can be frequently observed during summer...*

$$PCAPE_{bl} = -\frac{\tau_{bl}}{T_*} \int_{p|_{z=0}}^{p|_{z=z_b}} \left. \frac{\partial \overline{T}_v}{\partial t} \right|_{bl} dp \quad (6)$$

The surface buoyancy flux is used instead of the virtual temperature total tendency in the boundary layer forcing :

$$PCAPE_{bl} = -\frac{\tau_{bl} c_p \overline{\rho w' T'_v}|_{z=0}}{z_d} \quad (7)$$

where $\overline{\rho}$ is a reference density,

c_p is heat capacity at constant pressure,

z_d is the altitude of the departure level for convection (considered as the origin of updrafts).

$\overline{w' T'_v}|_{z=0}$ is the surface buoyancy flux :

$$\overline{w' T'_v}|_{z=0} = \frac{SHF}{\overline{\rho} c_p} + \left(\frac{R_v}{R_d} - 1 \right) \frac{\overline{T}|_{z=0} LHF}{\overline{\rho} L} \quad (8)$$

(SHF) the surface sensible heat flux,

(LHF) latent heat flux,

L is the latent heat of condensation and $\overline{T}|_{z=0}$ is the environment surface temperature.

R and R_v are gas constants for dry air and water vapor.

The used configurations are the ALADIN CMC configuration as described in Termonia et al. 2018

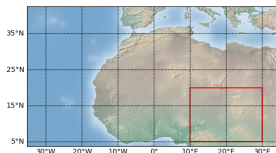
Parametrization	Operational configuration	Modified configuration
Radiation	RRTMG $\bar{L}W$, SW6 : Mlawer et al. 1997, Iacono et al 2008, Fouquart and Bonnel (1980)	RRTMG $\bar{L}W$, SW6 : Mlawer et al. 1997, Iacono et al 2008, Fouquart and Bonnel (1980)
Turbulence	CBR Cuxart et al. 2000, Bougeault et Lacarrere (1989)	CBR Cuxart et al. 2000, Bougeault et Lacarrere (1989)
Microphysics	Lopez 2002, Bouteloup et al. 2005	Lopez 2002, Bouteloup et al. 2005
Clouds	Smith 1990	Smith 1990
Sedimentation	Bouteloup et al. 2011	Bouteloup et al. 2011
Orographic gravity wave drag	Catry et al. 2008	Catry et al. 2008
Surface scheme	SURFEX	SURFEX
Shallow Convection	Bechtold et al. 2001	Bechtold et al. 2014
Deep Convection	Bougeault 1985	Bechtold et al. 2014

The activated subgrid processes in the operational and modified configurations

Tests with Moroccan ALADIN Operation model configurations

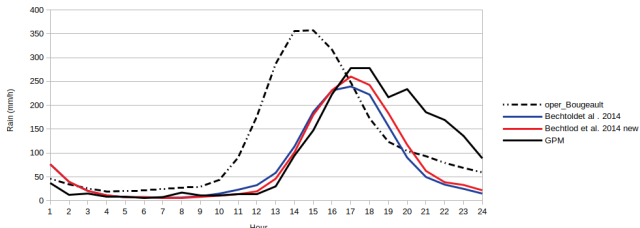
Two operational configurations are used :

	ALADIN-Morroco	ALADIN-NORAF
Resolution	7.5km	18km
Vertical levels	70	70
Model cycle	41t1	41t1
LBCs and initial state	ARPEGE	ARPEGE
Precipitation Diurnal cycle	first 24hours	first 24hours



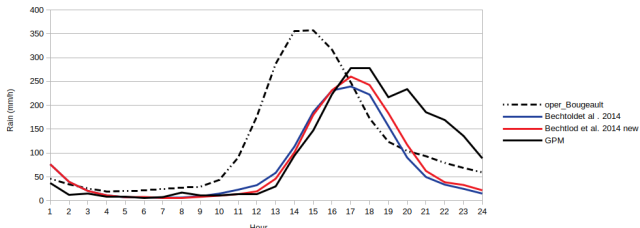
On the left : ALADIN-Morrocco domain with special focus on an Atlas mountain region. On the right : ALADIN-NORAF domain with the study sub-domain in red : Sahel (5N-20N,10E-30E)

First Results : Impact of the reformulation of the boundary layer forcing on diurnal cycle against GPM (Global Precipitation measurements) and AROME2.5km

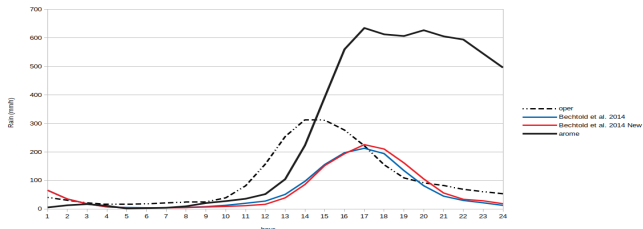


Experiments Vs GPM : Atlas mountain region, summer precipitation (20/08/2019-10/09/2019)

First Results : Impact of the reformulation of the boundary layer forcing on diurnal cycle against GPM (Global Precipitation measurements) and AROME2.5km

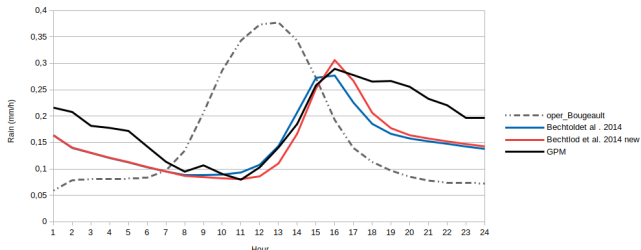


Experiments Vs GPM : Atlas mountain region, summer precipitation (20/08/2019-10/09/2019)



Experiments Vs AROME2.5 over the same region and the same period

First Results : Impact of the reformulation of the boundary layer forcing on diurnal cycle against GPM (Global Precipitation measurements)



Sahel (5N-20N,10E-30E), JJA 2019.

- The new formulation of the boundary layer forcing improved the diurnal cycle of precipitation when compared to GPM in the ALADIN-ARPEGE physics.
- There is no need to have a scaling parameter in the $PCAPE_{bl}$ computing.
- First tests on the ocean are ongoing with the hope to harmonize the boundary layer adjustment time scale between ocean and land.



Bechtold, P., N. Semane, P. Lopez, J.-P. Chaboureau, A. Beljaars, and N. Bormann, 2014 : Representing equilibrium and nonequilibrium convection in large-scale models. *J. Atmos.*



Termonia, P. and Fischer, C. and Bazile, E. and Bouyssel, F. and Brožková, R. and Bénard, P. and Bochenek, B. and Degrauwe, D. and Derková, M. and El Khatib, R. and Hamdi, R. and Mašek, J. and Pottier, P. and Pristov, N. and Seity, Y. and Smolíková, P. and Španiel, O. and Tudor, M. and Wang, Y. and Wittmann, C. and Joly, A., The ALADIN System and its canonical model configurations AROME CY41T1 and ALARO CY40T1, *GMD* 2018, 11, 257–281.



Bougeault, P. : A simple parameterization of the largescale effects of cumulus convection, *Mon. Weather Rev.*, 113, 2108–2121.1985.



El Khalki, E., Trambly, Y., Amengual, A., Homar, V., Romero, R., Saidi, M. E. and Alaouri M. : Validation of the AROME, ALADIN and WRF Meteorological Models for Flood Forecasting in Morocco. *Water*, 2020, 12,437.



Tiedtke, M., 1989 : A comprehensive mass flux scheme for cumulus parametrization in large-scale models. *Mon. Wea. Rev.*, 117, 1779–1800.



Bechtold, P., J.-P. Chaboureau, A. Beljaars, A. K. Betts, M. Kohler, M. Miller, and J.-L. Redelsperger, 2004 : The simulation of the diurnal cycle of convective precipitation over land in a global model. *Quart. J. Roy. Meteor. Soc.*, 130, 3119–3137.



Watters, D., Battaglia, A. and Allan R. P., The Diurnal Cycle of Precipitation According to Multiple Decades of Global Satellite Observations, Three CMIP6 Models, and the ECMWF Reanalysis. *Journal of Climate*, 2021, 1-58

Thank you for your attention